ACS OMEGA

Open Access

http://pubs.acs.org/journal/acsodf

Article

CO_2-Responsive Low Molecular Weight Polymer with High Osmotic Pressure as a Draw Solute for Forward Osmosis

Maedeh Ramezani, Sarah N. Ellis, Anna Riabtseva, Michael F. Cunningham,* and Philip G. Jessop*

Cite This: *ACS Omega* 2023, 8, 49259−49269

Read Online

ACCESS | Metrics & More | Article Recommendations | Supporting Information

ABSTRACT: A key challenge in the development of forward osmosis (FO) technology is to identify a suitable draw solute that can generate a large osmotic pressure with favorable water flux while being easy to recover after the FO process with a minimum of energy expenditure. While the CO_2- and thermo-responsive linear poly(*N*,*N*-dimethylallylamine) polymer (l-PDMAAm) has been reported as a promising draw agent for forward osmosis desalination, the draw solutions sufficiently concentrated to have high osmotic pressure were too viscous to be usable in industrial operations. We now compare the viscosities and osmotic pressures of solutions of these polymers at low and high molecular weights and with/without branching. The best combination of high osmotic pressures with low viscosity can be obtained by using low molecular weights rather than branching. Aqueous solutions of the synthesized polymer showed a high osmotic pressure of 170 bar under CO_2 (π_{CO2}) at 50 wt% loading, generating a high water flux against NaCl feed solutions in the FO process. Under air, however, the same polymer showed a low osmotic pressure and a cloud point between 26 and 33 °C (depending on concentration), which facilitates the recovery of the polymer after it has been used as a draw agent in the FO process upon removal of CO_2 from the system.

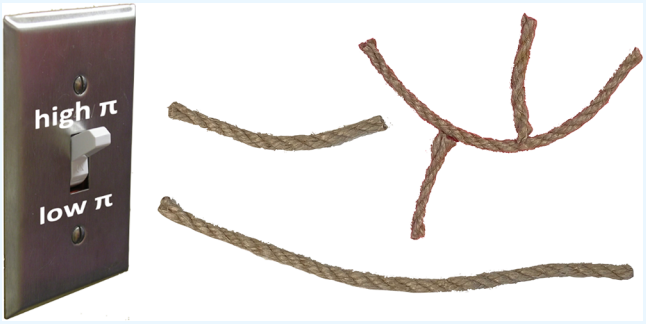

1. INTRODUCTION

Freshwater scarcity is one of the three global systemic risks (economic growth, water security, and ecosystem health) and a significant threat to ecosystems and public health in the twenty-first century.[1−3] Wastewater management through recovery and recycling has become an alternative strategy for addressing freshwater scarcity and minimizing the environmental risk of discharged wastewater on ecosystems and public health.[4,5] Moreover, recycling wastewater can reduce the pressure on ecosystems through minimizing freshwater withdrawal and can, therefore, contribute to water sustainability.

Membrane-based technologies such as membrane desalination, nanofiltration, reverse osmosis (RO) and forward osmosis (FO) are practical water purification methods.[6−9] FO utilizes an osmotic pressure difference across a semipermeable membrane to purify water from wastewater or seawater at low or no hydraulic pressures with high rejection of a wide range of contaminants and smaller membrane fouling propensity.[10−12] Unlike other membrane processes for water purification, the energy-consuming step in FO is not the osmosis step itself but rather the draw agent regeneration step. The draw agent must therefore be chosen carefully to minimize the energy cost of the regeneration step while still meeting osmosis-related requirements like high osmotic pressure, little to no reverse salt flux, and low viscosity. Moreover, a suitable draw solute must have low toxicity or ecotoxicity and must not degrade the FO membrane.[13−15]

Gases,[16] volatile compounds,[10,17] organics,[18,19] inorganic salts,[20,21] and functionalized nanoparticles[22−25] are the most reported draw agents for FO. Although these compounds can offer high osmotic pressure, they pose some challenges for FO desalination such as reverse solute flux and an energy-consuming regeneration process, particularly in traditional draw solutes.[1,26−28] To facilitate regeneration, stimuli-responsive draw agents have been developed. In other words, the osmotic pressure, solubility, and/or physical location of draw agents can be controlled by triggers such as pH, temperature, magnetic field, and CO_2.[29−33] Among these various triggers, CO_2 has the advantages of being nontoxic, inexpensive, and readily removable, unlike pH-responsive systems that require corrosive and accumulating acids/bases.[34] In water, CO_2-responsive agents such as CO_2-switchable polymers, molecules, and hydrogels can reversibly switch between protonated and deprotonated states when CO_2 is added or removed. This switching gives them controllable hydrophilicity, solubility, and swelling in water. This CO_2-responsive control of hydro-

Received: October 2, 2023
Revised: November 17, 2023
Accepted: November 23, 2023
Published: December 13, 2023

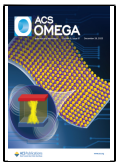

https://doi.org/10.1021/acsomega.3c07644
ACS Omega 2023, 8, 49259−49269

philicity can be used to facilitate draw agent removal from recovered water.

Recently, we reported a series of CO_2-switchable polymers as potential draw agents, including linear poly(*N*-methylethylenimine) (l-PMEI), branched poly-(*N*-methylethylenimine) (b-PMEI), and linear and branched poly(*N*,*N*-dimethylallylamine) (PDMAAm).[35,36] The initial purpose was to design a polymer that could show CO_2 switchability with a high osmotic pressure π_{CO2} under CO_2 and a low osmotic pressure π_{air} under air and that could be easily removed from a diluted draw solution simply by removing CO_2 followed by either precipitation or RO.

Although PMEI showed a high osmotic pressure under CO_2 (π_{CO2}: 67 bar at 43 wt/vol %), the polymer also exhibited high π_{air} (26 bar at the same concentration). Linear poly(*N*,*N*-dimethylallylamine) l-PDMAAm showed the greatest contrast between its osmotic pressure in the presence of CO_2 (π_{CO2}: 59.2 bar at 33 wt/vol % loading) versus under air (π_{air}: 2.3 bar). In addition, uncharged l-PDMAAm (35 wt/vol %) showed a cloud point at 24 °C, which could facilitate the removal of the polymer from purified water.[35] However, the viscosities of aqueous solutions of l-PDMAAm were too high to allow the practical use of this polymer as a draw agent. The use of branched versions of b-PDMAAm did not significantly reduce the viscosity or improve the solubility at high concentration.[35,36] Considering our previous work, we hypothesized that shorter chain polymers could (a) allow greater loadings and therefore higher osmotic pressure π_{CO2} and (b) yield less viscous solutions that could solve the existing challenges of limited solubility and high viscosity at high concentration, thus enabling the polymer to exhibit its highest potential osmotic pressure at high concentrations without excessive viscosity. On the other hand, there is a risk that the use of shorter chains might make the subsequent polymer recovery by precipitation less complete.

The key influential factors of the FO separation performance are osmotic pressure (or osmolality), solubility in water, and viscosity.[37,38] For example, Cai et al. compared poly(2-(dimethylamino)ethyl methacrylate) (PDMAEMA) with number average molecular weights of 4000, 9000, and 13,000 g/mol (P4000, P9000, and P13,000) as CO_2-responsive draw solutes for FO desalination. The results showed that the osmolality of the polymer draw solutes in carbonated water increased with decreasing molecular weight and exceeded >2.0 osmol/kg at 0.4 g/g for P4000 while the solubility of P9000 and P13,000 was limited to a concentration of 0.3 g/g.[39] Yasukawa et al. investigated nonstimuli-responsive neutral polymers (PEGs) with molecular weights of 106 to 8300 g/mol as draw solutes. They found that increasing the molecular weight of the PEG draw solute dramatically decreased the FO flux due to lower diffusivity of higher molecular weight polymer, resulting in severe internal concentration polarization (ICP).[40]

In this work, we demonstrate the osmotic pressure, viscosity variations, and FO performance of low molecular weight CO_2-switchable linear poly(*N*-dimethylallylamine) l-PDMAAm polymer as a draw solute to address the challenges of limited solubility and high viscosity, which resulted in low osmotic pressures and low water flux with the higher molecular weight linear analogs in carbonated water. After the FO process and CO_2 removal from the system, the polymer was recovered from the diluted draw solution by slight heating of the solution above the lower critical solution temperature (LCST), resulting in >99% recovery of the polymer. Scheme 1 illustrates the FO process using this CO_2-switchable thermoresponsive polymer as a draw solute.

Scheme 1. CO_2-Switchable Thermoresponsive-FO Desalination System.

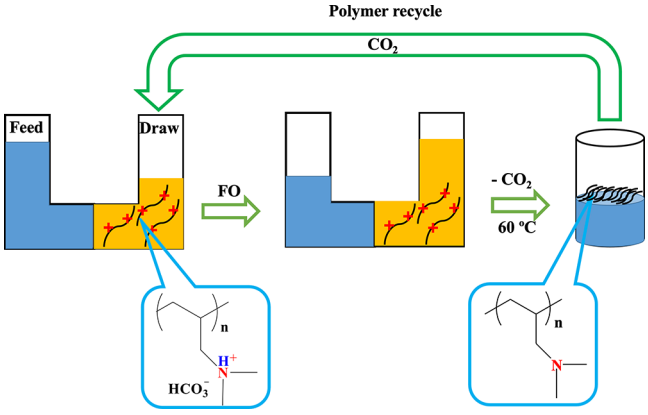

2. EXPERIMENTAL METHODS

2.1. Materials and Instruments. *N*,*N*-Dimethylacrylamide (DMA, 99%) was obtained from Millipore-Sigma and passed through an inhibitor removal column before use. *tert*-Dodecanethiol (trDDT, 98.5%), 4-methylmorpholine (99%), lithium aluminum hydride pellets ($LiAlH_4$, 95%) and anhydrous magnesium sulfate were obtained from Millipore-Sigma and used as received. 2,2′-Azobis(2-methylpropionitrile) (AIBN) was obtained from Millipore-Sigma and recrystallized from methanol before use. Ethyl acetate (99.8%), hexanes (99%), and toluene (99.8%) were obtained from Fisher Scientific and used as received. Deionized water with a resistivity of 18.2 MΩ·cm (before exposure to air) was obtained from a Synergy Millipore system. CO_2 (supercritical chromatographic grade, 99.998%, Praxair) was used as received.

UV−vis spectroscopy (Agilent Technologies, Cary 300 Bio temperature controlled spectrometer) was used to determine the cloud points and the LCST of low molecular weight linear PDMAAm. Cloud point measurements were performed to identify the temperature at which the transmittance drops to ∼0%, where phase separation is initiated and the transparent solution changes to a cloudy solution. The kinematic viscosity of polymer solutions at different concentrations was measured by using a Cannon-Fenske-type viscometer (tube size 350) at 25 °C.

The osmotic pressures of polymer solutions were measured at different concentrations under air and CO_2 atmosphere, at room temperature (23 ± 1 °C) using a membrane osmometer designed by Grattoni,[41] with Dow BW30 membranes. The solution chamber was hermetically sealed, confining the solution to a fixed volume of 12 mL. The chamber was designed to promote the complete escape of air during solution loading. The polymers were rigorously lyophilized before solutions were prepared to ensure that the polymers were completely dry. Polymer solutions were carbonated at 1 bar by bubbling CO_2 (flow rate 100 mL/min) through the solutions for up to 5 h.

The GPC analysis of low molecular weight linear poly(*N*,*N*-dimethylacrylamide) (PDMA) was performed using THF as

https://doi.org/10.1021/acsomega.3c07644
ACS Omega 2023, 8, 49259−49269

the eluent. Samples were prepared at 4 mg/mL and passed through a 0.2 μm filter prior to injection. The samples were analyzed on a Waters 2695 separation module equipped with a Waters 410 differential refractometer and Waters Styragel HR (4.6 × 300 mm) 4, 3, 1, and 0.5 separation columns at 32 °C and 1 mL/min flow rate. The GPC was calibrated using PS monodisperse standards. The GPC analysis of higher molecular weight linear and branched poly(*N*,*N*-dimethylacrylamide) (PDMA) was performed as described in our previous report.[36] ^{1}H NMR spectra were recorded at 298 K with a Bruker Avance 400 MHz NMR spectrometer. Polymer samples (l-PDMA and 1-PDMAAm) were dissolved in NMR solvents (D_2O, $CDCl_3$).

FTIR spectra were measured by using a Bruker ALPHA FTIR Spectrometer with an attenuated total reflectance (ATR) sampling module. Polymer samples were analyzed without using a solvent or dilution.

2.2. Synthesis of Polymers. Linear poly(*N*,*N*-dimethylallylamine) was synthesized by polymerization of DMA followed by reduction of the resulting polymer l-PDMA. In a typical method, DMA (3.0 mL, 29 mmol) and trDDM (0.60 mL, 2.9 mmol) were dissolved in 50 mL of toluene and the resulting solution added to a 100 mL flask. The argon was purged into the solution for 10 min, and then AIBN (60 mg, 0.29 mmol) was added to the flask. The mixture was again purged for 10 min and then heated to 60 °C with stirring at 420 rpm. After 6 h, the flask was cooled to room temperature (23 ± 1 °C). The resulting l-PDMA polymer (a white powder) was purified from residual monomers by reprecipitation from toluene with hexanes and dried in a vacuum oven at 50 °C overnight (yield: 77%).

To synthesize l-PDMAAm from l-PDMA, a three-necked round-bottom flask containing a stir bar and 3.86 g of $LiAlH_4$ (pellets, 0.1 mol) was fitted with a condenser and rubber septum and degassed by three cycles of pumping and N_2 backfilling. Then, under flowing N_2, 100 mL of 4-methylmorpholine was quickly added to the flask. The mixture was heated to 68 °C with vigorous stirring at 850 rpm to disperse $LiAlH_4$ into the solvent. After complete dispersion, 10 g of dissolved l-PDMA (0.1 mol of repeat units) in 80 mL of 4-methylmorpholine was dropped slowly into the flask through a syringe. After 24 h, 50 mL of THF was added slowly into the mixture and the temperature and stirring were maintained for another 24 h.

In the next step, the flask was cooled to room temperature (23 ± 1 °C) and transferred into an ice bath. After cooling, deionized water (6.0 mL) was added dropwise under N_2, followed by 15 wt % sodium hydroxide solution (6.0 mL) and then more water (10 mL). (Caution: due to the strong reaction with $LiAlH_4$ and the resulting hydrogen gas formation, water must be added very slowly with continuous flushing of N_2 through the flask until complete quenching of $LiAlH_4$ has been achieved.)[35,36] The flask was warmed to room temperature (23 ± 1 °C) and left stirring overnight. Anhydrous magnesium sulfate was added until it clumped at the bottom of the flask. The solid phase was removed by gravity filtration and washed twice with ethyl acetate. The filtrate and washings were evaporated to dryness under vacuum, leaving behind a transparent yellow solid (Yield: 88%).

Branched PDMA was synthesized through conventional free-radical copolymerization of DMA monomer with *N*,*N*′-methylenebisacrylamide (MBA) as the branching agent and trDDT as the chain transfer agent with a AIBN:MBA:trDDT mole ratio of 1:1:3. The procedure for reducing b-PDMA to b-PDMAAm was similar to that described above for the linear polymer.[36]

2.3. Forward Osmosis Process. The FO tests were carried out using glassware equipment of different scales, as shown in Figure S1. Commercially available FTS H_2O cellulose triacetate FO flat sheet membranes (Sterlitech) were used. According to the manufacturer (Sterlitech), the reverse salt flux of NaCl in this kind of membrane is smaller than 2 g/m^2·h (H_2O vs 1 M NaCl in FO). The membrane was a circular shape of 4.7 cm diameter, soaked in the feed solution (NaCl) for a minimum of 1 h before use. The feed and draw sides were connected via flanges with an internal diameter of 2.5 cm. The flanges were wrapped with Teflon tape to prevent leaking during the FO process, and the membrane was placed between flanges. A 50 wt % solution of l-PDMAAm was carbonated with bubbling CO_2 for at least 25 min before the FO process. NaCl solutions with different concentrations (0.2, 1.75, and 3.5 wt %) were used as the feed and stirred at 500 rpm during the FO process. The active layer of the membrane faced the draw solution in all experiments. The conductivity of the feed solution was recorded during the FO test and was used to calculate the flux as a function of the volume and time (LMH). For this purpose, the conductivity probe (Thermo Scientific Orion 013005MD) was calibrated with NaCl standard solutions. The volume reduction of the feed was calculated from the concentration variation over time to obtain the volume of transferred water from the feed to the polymer side.

After the FO process, a temperature increase (e.g., 55 °C) was employed to remove CO_2 from the diluted draw solution. This temperature rise also triggered the precipitation of the polymer, causing the neutral polymer to form a separate phase from the solution. The bulk polymer was collected, and the process was then followed by filtration using a 0.22 μm syringe filter.

An RO bench-scale experimental setup was also used as a polishing step to remove residual traces of polymer from the water-rich phase and produce clean water. The RO setup (Sterlitech HP4750 High Pressure Stirred Cell) had a cell width of 14.6 cm, a high-pressure coupling, and a commercially available stainless steel cross-flow membrane filtration unit equipped with a 14.6 cm^2 active membrane area and PTFE stir bar connected to a N_2 tank.

3. RESULTS AND DISCUSSION

3.1. Synthesis and Characterization of CO_2-Switchable Polymers. Linear and branched poly(*N*,*N*-dimethylacrylamide) samples with different molecular weights (linear: M_w = 3.2 and 18.5 kDa, branched: M_w = 20.8 kDa) were synthesized using free-radical polymerization in the presence of a chain transfer agent (CTA) to control the polymer growth and prevent gelation. To produce linear poly(*N*,*N*-dimethylallylamine) l-PDMAAm, the acrylamide groups in the l-PDMA polymer were reduced by using $LiAlH_4$. Although there are two steps in the synthetic procedure to obtain the final l-PDMAAm product, which might raise the economic and environmental cost compared to polymers that can be made in a single step, the CO_2 switchability and thermoresponsivity of the polymer make it an easily recoverable and reusable draw agent. It is also possible to prepare the polymer by polymerizing allylamine hydrochloride and then methylating with formic acid/formaldehyde, thereby avoiding the use of

https://doi.org/10.1021/acsomega.3c07644
ACS Omega 2023, 8, 49259−49269

$LiAlH_4$.[42] Scheme 2 shows the linear and branched structure of PDMAAm polymers in this study.

Scheme 2. Linear and Branched PDMAAm Polymers in This Study

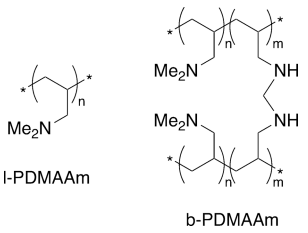

Successful polymerization was confirmed by Fourier transform infrared spectroscopy (FTIR) and ^{1}H NMR spectroscopy, which confirmed the reduction to the tertiary amine. Figure 1 compares the ^{1}H NMR and FTIR spectra of the low molecular weight l-PDMAAm polymer to those of l-PDMA from which it was made.

The FTIR spectrum of l-PDMA (Figure 1A) shows the amide carbonyl stretching band at 1690 cm^{-1}; the disappearance of this band in the spectrum of the l-PDMAAm confirms the successful reduction of the amide groups.[36] ^{1}H NMR spectroscopy also confirmed the successful reduction of amide groups in l-PDMA to the amine through the disappearance of the signal corresponding to the hydrogen neighboring the C═O of the amide at 2.6 ppm.[35]

The solubility of l-PDMAAm in carbonated water was confirmed by bubbling CO_2 into the mixture of polymer and water solution until equilibrium was reached. Figure S2 shows the conductivity measurement of the polymer solution at 35 wt % as a function of CO_2 bubbling. Initially, the conductivity of the mixture is low (58.6 μS/cm), due to the low solubility of the polymer in water under air. Upon the bubbling of CO_2 into the mixture, the nitrogen atoms are protonated and hence increase the solubility of polymer in the carbonated water, resulting in an increased conductivity until equilibrium is reached at 8590 μS/cm.

3.2. Osmotic Pressure. In FO desalination, an osmotically driven process, careful selection of the draw agents dissolved in water plays a critical role in determining the FO efficiency. A successful draw solute must exhibit a high solubility in water with high osmotic pressure compared to the feed solution in order to generate high and efficient water flux across the semipermeable membrane.[42,43] In this work, we studied the osmotic pressure of three kinds of PDMAAm polymers including linear low and high molecular weight and branched polymers. Table 1 shows the molecular weights of the studied polymers. In addition, the molecular weight distributions of linear and branched polymers are shown in Figure S3. As expected, the low molecular weight polymer contains more very small polymer chains compared to the linear high molecular weight and branched polymers.

Table 1. Molecular Weights of PDMAAm in This Study

sample	M_n (kDa)	M_w (kDa)	Đ
linear, low M_w	2.5	3.2	1.3
linear, high M_w	8.0	18.5	2.3
branched	5.9	20.8	3.5

The osmotic pressure of CO_2-responsive PDMAAm polymers was measured under air (π_{air}) and in the presence of CO_2 (π_{CO2}) using direct membrane osmometry, which is capable of direct measurement of osmotic pressure without further calculation, as reported previously.[35,36] For concentrated solutions, osmotic pressures measured directly by membrane osmometry tend to be lower than those calculated from freezing point or vapor pressure lowering measurements,[44] possibly due to ICP, but might be more representative of the effective osmotic pressures experienced in FO processes where ICP is also likely to occur. Figure 2 shows the osmotic pressure of branched and linear polymers under air and CO_2 at different concentrations. At low concentrations (<20 wt %), the osmotic pressure of all

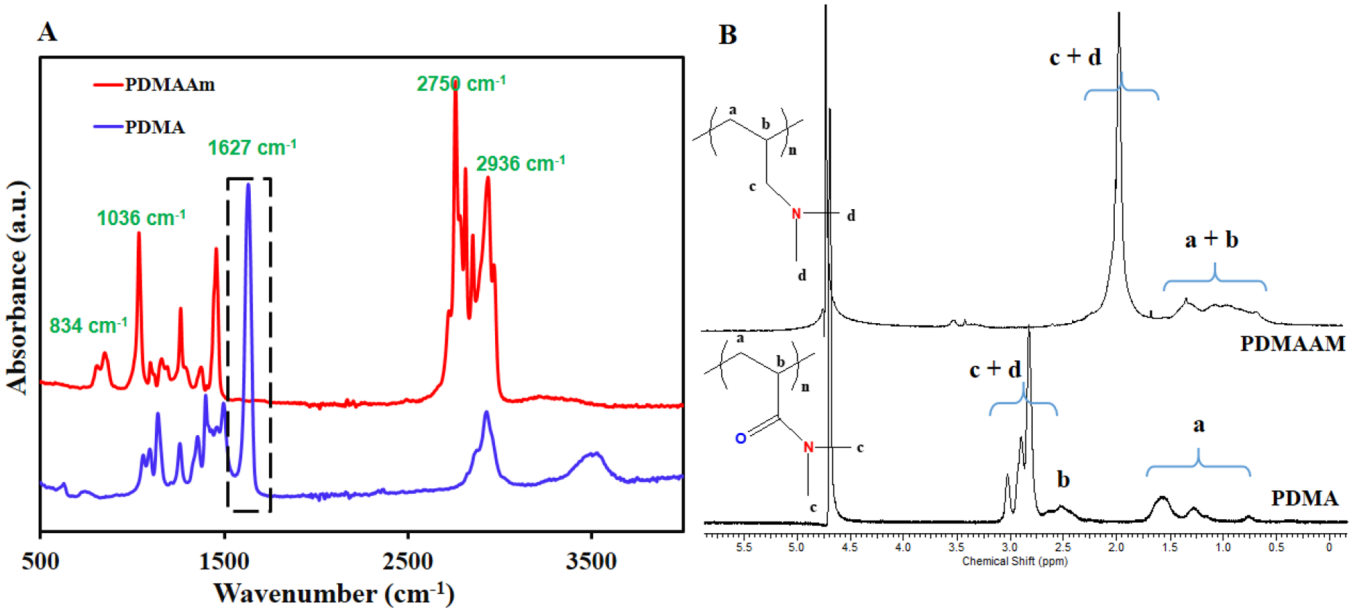

Figure 1. Characterization of the l-PDMA and l-PDMAAm polymers: (A) FTIR spectra; (B) ^{1}H NMR spectra in D_2O.

https://doi.org/10.1021/acsomega.3c07644
ACS Omega 2023, 8, 49259−49269

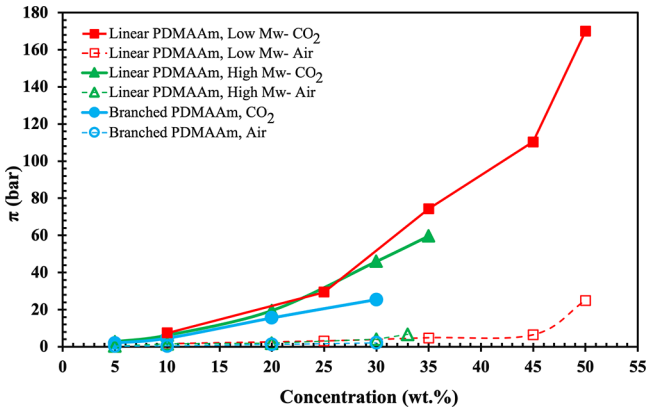

Figure 2. Osmotic pressure of l-PDMAAm and b-PDMAAm polymers as a function of their concentration in water, under air and CO_2.

polymers under CO_2 is independent of the molecular weight and the structure of the polymer.[45] However, at intermediate concentrations ~20−30 wt %, the two linear l-PDMAAm polymers appear to have approximately the same osmotic pressure π_{CO2} but the branched b-PDMAAm shows a lower osmotic pressure π_{CO2}, presumably due to the additional interactions between branches of one macromolecule (intramolecular polymer−polymer interaction).[36] At concentrations above 30 wt %, the low molecular weight and high molecular weight linear l-PDMAAm polymers have different osmotic pressures, with the low molecular weight polymer giving superior pressures. The reason can be related to the effective parameters of linear polyelectrolytes in solution, such as interactions between polymer and solvent, polyions and/or counterions, flexibility of the polymer chains, and counterion distribution.[45] In the lower molecular weight polymers, the interaction between the polyions and counterions may be increased due to a less repulsive effect between positive charges and less neighboring interaction between $H^+N(R)_2$ groups in polymer segments. The previous result showed that in tertiary amine polymers with high nitrogen-to-carbon ratios, such as l-PDMAAm as polar aprotic polymers, at the critical concentration, polymer−water interactions are more favorable than polymer−polymer interactions. Above this concentration, the repulsion is stronger between the polymer chains resulting in pulling more water to reduce the chains' repulsion, which causes an increase in the osmotic pressure.[35] Therefore, the osmotic pressure π_{CO2} of low molecular weight l-PDMAAm significantly increased above 170 bar at 50 wt %. The osmotic pressure above 35 wt % for branched and high molecular weight linear l-PDMAAm solutions could not be measured due to their high viscosity.[35,36]

CO_2-responsive draw agents also ideally should have a low osmotic pressure in air to facilitate the separation of the draw solute from water. In other words, a large difference between (or even better a large ratio of) the osmotic pressures π_{CO2} and π_{air} will provide easy separation of the CO_2-switchable draw solute from the diluted draw solution if an RO or nanofiltration step is used either as the primary method for recovering the polymer or as a polishing step to remove residual polymer after precipitation and filtration. As shown in Figure 2, PDMAAm polymers with branched and linear structures exhibited low π_{air}, which allowed easier separation of the polymers from water. In addition, the osmotic pressure of synthesized l-PDMAAm compared to those of the other polymers and small molecules as draw agents reported in the literature is shown in Table 2.

Table 2. Comparison of the Osmotic Pressures of Draw Agents from the Literature

draw agent	concentration	osmotic pressure	ref.
P_{4444} DMBS[a]	70 wt %	25 bar[b]	11
P_{4444} TFA[c]	70 wt %	38 bar[b]	11
polyethylene glycol[d]	40 wt %	50 bar[e]	46
PAGB[f]	40 wt %	20 bar[e]	46
ethylene oxide-propylene oxide copolymer[g]	70 wt %	96 bar[e]	47
PAANa[h]	0.12 g/mL	8.1 bar[i]	48
PSSS-PNIPAM[j]	33.3 wt %	28.6 bar[k]	49
trimethylamine[l]	1.0 M	48.8 bar[l]	50
l-PDMAAm	50 wt %	>170 bar[m]	This work

[a]P_{4444} = tetrabutylphosphonium, DMBS = 2,4-dimethylbenzene sulfonate. [b]Measured by vapor pressure osmometer. [c]TFA = trifluoroacetate. [d]M_w = 4000 g/mol. [e]Measured by water activity method. The water activity aw of the DS solutions at 25 ± 1 °C was measured using a water activity meter. [f]PAGB = poly (propylene glycol-ran-ethylene glycol) monobutyl ether, M_w = 4000 g/mol. [g]Ethylene oxide-propylene oxide copolymer, M_w = 2000 g/mol. [h]PAA Na= poly(acrylic acid) sodium salts, M_w = 1800 g/mol. [i]The osmolality of draw solutions was converted to osmotic pressure using a model 3250 osmometer. [j]PSSS-PNIPAM = poly(sodium styrene-4-sulfonate-co-n-isopropylacrylamide), 15 wt % SSS. [k]Measured by direct membrane osmometer. [l]Measured by a stream analyzer, under CO_2. [m]Under CO_2.

The viscosity of the draw solution is the other critical factor that can significantly affect the FO process and osmotic pressure. Draw solutions with high viscosity can show external concentration polarization (ECP) in the solution next to the membrane, which causes a reduction in the water flux. Excessive viscosity also increases the energy cost of pumping the solution through the system.[12] Figure 3 shows the kinematic viscosity of low and high molecular weight PDMAAm solutions at different concentrations under CO_2 and air. At low concentrations of ≤20 wt %, all samples show approximately the same viscosity under CO_2 and air, which shows that viscosity at dilute concentration is independent of molecular weight and structure of PDMAAm.[44] However, at intermediate concentrations of 20−30 wt %, both high molecular weight linear and branched b-PDMAAm show a significant increase from 30 cSt at 20 wt % to ~740 and ~1500 cSt at 30 wt % under CO_2, while the viscosity of the low molecular weight linear l-PDMAAm appears to have risen to only ~50 cSt at 30 wt %. Upon further increase in concentration to >30 wt % for higher molecular weight polymers, the viscosity increases exponentially above 4000 (branched) and 40,000 cSt (linear), respectively, at 40 wt %, while the low molecular weight polymer shows a less drastic increase in viscosity (500 and 1500 cSt at 45 and 50 wt % respectively), demonstrating the viscosity-lowering benefit of using lower molecular weight l-PDMAAm.[36]

3.3. Cloud Point. If the neutral polymer is thermoresponsive, then changing the temperature of a noncarbonated aqueous solution of the polymer in order to initiate precipitation could provide an energy-efficient regeneration mechanism in the FO process. Temperature is the most widely

https://doi.org/10.1021/acsomega.3c07644
ACS Omega 2023, 8, 49259−49269

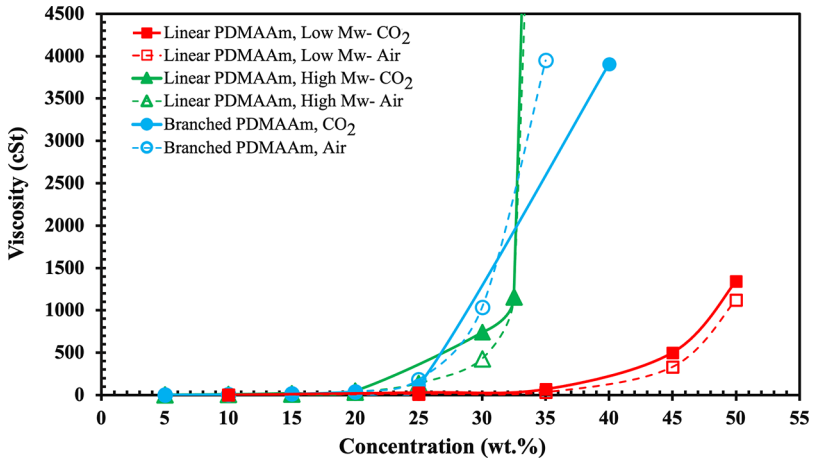

Figure 3. Kinematic viscosity of linear and branched PDMAAm solutions in water as a function of their concentration under air and CO_2.

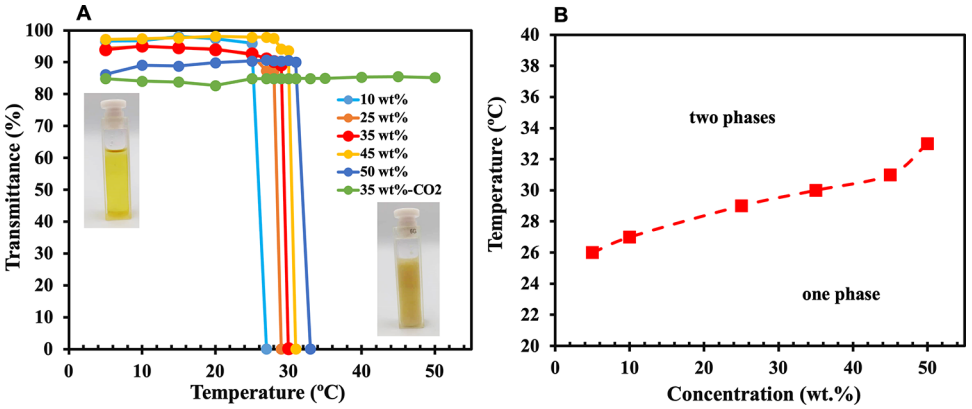

Figure 4. (A) Transmittance of aqueous mixtures of l-PDMAAm (linear low M_w) as a function of concentration under air or, for the green line only, under CO_2. (B) Cloud point of l-PDMAAm solutions in water as a function of their concentration under air. Solutions are biphasic (solid +liquid) above the curve and monophasic (liquid) below the curve.

used trigger in stimuli-responsive polymeric systems.[51−59] Unfortunately, a polymer that is responsive to only temperature is unlikely to generate high osmotic pressures because thermoresponsive polymers are of medium hydrophilicity. Very hydrophilic polymers, which are the polymers most likely to generate very high osmotic pressures, either are not thermoresponsive or have prohibitively high LCST. Thus, a polymer that is both thermoresponsive and CO_2-responsive makes it possible to achieve both high osmotic pressure and facile recovery and regeneration.

A cloud point is the temperature at which a polymer in an aqueous solution precipitates. The cloud point varies depending on the concentration of the polymer in the water. The lowest cloud point is called the LCST.[60−67] For example, poly(*N*-isopropyl acrylamide) (PNIPAM) is the most studied thermo-sensitive polymer; it has a sharp LCST in water at around 32 °C.[31,68,69] Table S1 shows the LCST of the thermoresponsive polymers reported in the literature.

Many polymers are undesirable as draw solutes, because they have no LCST, a high LCST necessitating a high temperature to be recovered from water, or a very low LCST (below or at room temperature). A low LCST can cause an issue during the FO process, because the system would need to be cooled during the FO process to prevent the precipitation of polymers while running the FO process.[61] A CO_2-switchable polymer with a low LCST or essentially complete insolubility in noncarbonated water, in our experience, takes a long time to dissolve in carbonated water, which would be unacceptable in a practical process. For these reasons, a polymer with a medium LCST is preferable, meaning one that is 10 or 20 °C above room temperature.

In this work, synthesized l-PDMAAm polymers display both thermoresponsiveness and CO_2 switchability. Figure 4 shows the cloud point temperatures of low molecular weight l-PDMAAm at different concentrations in the absence of CO_2. The polymer solution has a sharp cloud point at varying concentrations (33 °C at 50 wt % versus 26 °C at 10 wt %). Although the polymer shows a low cloud point at dilute concentrations under air (26 °C at 10 wt %), the carbonated solution remains transparent at all temperatures in the studied range (5 to 50 °C), indicating that the polymer would remain soluble in carbonated water during the FO process, and there would be no need for cooling.

3.4. FO Desalination. A laboratory-scale FO glassware apparatus was used to test the synthesized low molecular weight l-PDMAAm as the draw agent for FO. Based on the measured osmotic pressures of the polymer solutions, 50 wt % solution of the polymer in carbonated water was selected as the draw solution for the FO test. The polymer was mixed with an equal mass of water and carbonated with 1 bar of CO_2. The carbonated l-PDMAAm polymer solution was placed into the draw side of the FO apparatus against the active layer of the

https://doi.org/10.1021/acsomega.3c07644
ACS Omega 2023, 8, 49259−49269

cellulose triacetate membrane and across from the feed NaCl solution. The flux was monitored by measuring the change in the conductivity in the feed solution.

Figure S4 shows the feed solution conductivity as a function of time during the FO process. As the graphs show, as water crossed from the feed to the draw side, the concentration of the feed NaCl solution increased over time, and therefore, its conductivity increased. Figure 5 shows the water flux as a function of time for feed solutions with different initial salinities.

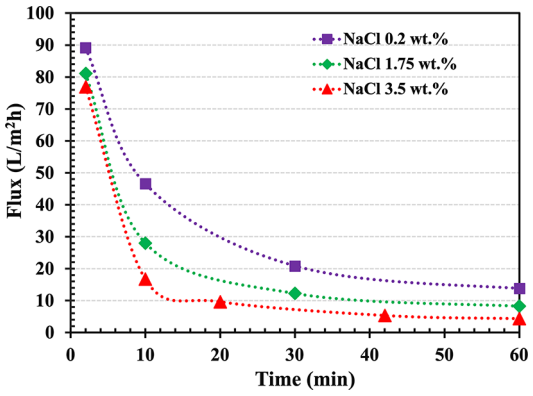

Figure 5. Measured water flux (L $m^{-2}h^{-1}$) over time as a function of the initial feed concentration. In all cases, the draw solution initial concentration was 50 wt % l-PDMAAm (low M_w) in carbonated water.

As shown in Figure 5, the highest water flux of 89 L m^{-2} h^{-1} was measured for 0.2 wt % of NaCl feed solution while slightly lower initial water fluxes of 81 and 77 L m^{-2} h^{-1} were observed from 1.75 and 3.5 wt % NaCl solutions, respectively. According to our previous study, high molecular weight l-PDMAAm at a concentration of 30 wt % showed an initial water flux of only 30 L m^{-2} h^{-1} against 1.75 wt % NaCl feed solution.[34] The total amount of water that crossed the membrane from the feed solutions to the draw side is shown in Figure S5. After 3 h, 9.0, 5.0, and 2.5 mL of water permeated from 0.2, 1.75, and 3.5 wt % NaCl feed solutions into the draw solution, respectively.

Decline in water flux over time is a common phenomenon in batch FO experiments due to dilution of the draw, concentration of the feed, and in some cases the occurrence of ECP, which arises from the unstirred diffuse boundary layer on the active layer side of the FO membrane.[12,59,60] In other words, permeation of water into the draw side dilutes the portion of the draw solute that has close contact with membrane and therefore reduces the osmotic pressure difference across the membrane and hence decreases the water flux.[34,70] However, circulation during the FO process and controlling the hydrodynamic operating conditions can minimize the ECP.[12,71]

In another experiment, a larger apparatus was used for the FO test (as shown on the right in Figure S1). For this purpose, 45 g of polymer was dissolved into water (at 50 wt %) under a CO_2 atmosphere and the FO process was performed for a 3.5 wt % NaCl feed solution (Figure S8). While similar initial water flux was obtained (76 L m^{-2} h^{-1} against 3.5 wt % NaCl feed solution) compared to the small FO apparatus, the FO test was continued for 21 h until the top of the feed solution reached the top of the active layer (18 mL of water passed through the membrane during the FO process). Better circulation was provided by using a stir bar in the draw solution, although, on an industrial scale, circulation would be provided by pumps and forcing the solution through hollow fiber membranes providing efficient contact of the draw solution with the membrane and decreasing ECP. The initial FO water fluxes for the FO tests with different salinities, recycled polymer, and different sizes of FO apparatus are shown in Figure 6. In the future, pilot-scale runs will be appropriate for future studies and development.

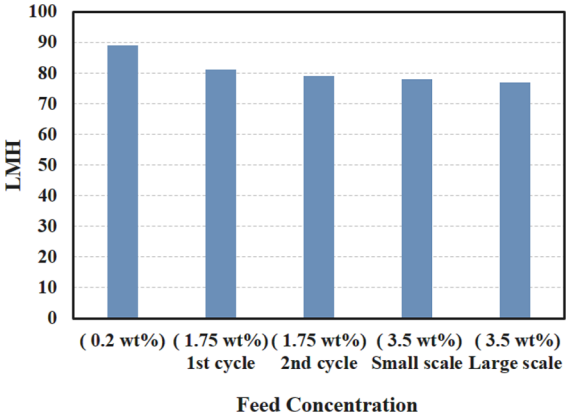

Figure 6. Initial water flux observed with draw solutions consisting of protonated low molecular weight l-PDMAAm polymer (50 wt%), as a function of NaCl feed solution concentration.

In a successful FO process, the back-diffusion or reverse salt flux (RSF) of draw solute through the membrane should be zero or negligible.[72] To evaluate whether RSF occurred, all feed solutions after FO experiments were analyzed by ^{1}H NMR and IR spectroscopy to detect any polymer that may have diffused into the feed side (Figure S7). Figure S7A shows the IR spectrum for feed and draw agent solution before and after the FO test of 3.5 wt % NaCl solution. No polymer peak was detected in the feed solution after the FO process, and only peaks due to water appeared in the spectrum. As the NMR result shows in Figure S7B, no polymer peaks were detected between 1 and 3 ppm (no polymer was also detected for the larger scale experiment after 21 h of the FO test).

To recover the polymer after the FO test, the diluted draw solution was heated slightly (e.g., 55 °C) under N_2 to remove CO_2 from the solution. l-PDMAAm displays sharp cloud points from 26 to 33 °C depending on the concentration. Therefore, heating the diluted polymer solution after the FO process to 50 °C for CO_2 removal also causes the neutral polymer to form a phase separate from the solution. Figure S8 shows the draw solution after the removal of CO_2. Although there might be a concern about the energy consumption that is required for the heating, the required temperature for CO_2 removal from the system is so low that low-grade waste heat would suffice.[42,73] The use of precipitation to recover the draw polymer also ensures that the polymer will be separated from any salt or other water-soluble impurities that may have migrated across the membrane from the feed during the FO step.

After the CO_2 removal, the mixtures were analyzed to measure the extent of phase separation. The precipitated polymer layer was gently removed using a spatula, and the aqueous phase was taken for further analysis. Two methods were applied in sequence to the water-rich phase to remove

https://doi.org/10.1021/acsomega.3c07644
ACS Omega 2023, 8, 49259−49269

any residual polymer remaining after removal of the bulk of the precipitated polymer. First, the aqueous solution was filtered with a 0.22 μm syringe filter. Figure S9 shows the ^{1}H NMR and FTIR spectra of the polymer-rich and water-rich phases after removing the remaining polymer from the aqueous solution by a syringe filter. As the result shows, there was a residual amount of ∼2 wt % l-PDMAAm in the water-rich phase (water ∼98 wt %) and residual amount of water ∼2 wt % in the polymer-rich phase (polymer ∼98 wt %, concentrations were measured by the ^{1}H NMR spectrum in acetone-D6 and DMF as an internal standard).

In another experiment, after the syringe filter step, RO was used as a post-treatment process to recover the small amount of dissolved polymer that was not separated from the water-rich phase and produce clean water. The osmotic pressure of the water-rich phase was found to be 6.9 bar, which showed that a slight amount of CO_2 still remained in solution, and therefore, some nitrogen atoms of the l-PDMAAm remained protonated and made the polymer slightly soluble in the water. To fix this problem, N_2 pressure was applied to force the water-rich phase through an RO system (150 psi) until the permeate was clean. Figure S10 shows the FTIR and ^{1}H NMR spectra of the aqueous solution before and after RO. No polymer was detected in the filtrate by ^{1}H NMR spectroscopy. The fact that some CO_2 remained suggests that more complete removal of the CO_2 might decrease the amount of residual polymer in the recovered water (and its osmotic pressure) and might even eliminate the need for an RO step.

CONCLUSIONS

We compared the performance of low molecular weight CO_2-switchable l-PDMAAm with that of high molecular weight linear and branched counterparts to evaluate them as draw agents for FO. We also compared the viscosity of solutions of these various polymers in carbonated or normal water. The carbonated solutions of the low molecular weight linear PDMAAm showed the greatest osmotic pressure, lowest viscosity, and highest solubility of the three polymers under CO_2, which could address previous challenges related to low solubility and high viscosity of the higher molecular weight and branched structures. In addition, the low molecular weight polymer was tested for the FO performance against NaCl feed solutions. The l-PDMAAm draw agents displayed improved initial water fluxes of 89, 81, and 77 LMH for 0.2, 1.75, and 3.5 wt % of NaCl feed solutions, respectively. After the FO step, regeneration of the draw solute was achieved by heating the diluted draw agent to remove CO_2 from the system. This resulted in the precipitation and thus facile recovery of the draw polymer from the dilute draw solution with minimum amount of the residual polymer ∼2 wt % in the water-rich phase. A subsequent RO step was able to remove the remaining residual polymer from the water-rich phase to obtain clean water.

ASSOCIATED CONTENT

Supporting Information

The Supporting Information is available free of charge at https://pubs.acs.org/doi/10.1021/acsomega.3c07644.

Lab-scale FO glassware apparatus; molecular weight distributions of polymers; conductivity plus IR and ^{1}H NMR spectrum of the draw agent and feed solution before and after the FO test; LCST of the thermoresponsive polymers/polyelectrolytes in water; conductivity as a function of time during the FO test after 3 h; volume of water passed through the membrane during the FO process with different initial feed NaCl concentrations using the small-scale apparatus; water flux (LMH) over the time using different-scale FO apparatus; IR spectrum of the draw agent solution before and after FO test and ^{1}H NMR spectrum of the feed solution of 3.5 wt % after the FO test; diluted draw solution after the FO test, phase separation after removing CO_2 from the mixture, and recovered l-PDMAAm; FTIR spectra and ^{1}H NMR spectra of the polymer-rich phase; and FTIR and ^{1}H NMR of the water-rich phase after the removal of CO_2 and the precipitated polymer from the diluted draw solution (PDF)

AUTHOR INFORMATION

Corresponding Authors

Michael F. Cunningham − *Department of Chemical Engineering, Queen's University, Kingston, ON K7L 3N6, Canada*; Email: michael.cunningham@queensu.ca

Philip G. Jessop − *Department of Chemistry, Queen's University, Kingston, ON K7L 3N6, Canada*; orcid.org/0000-0002-5323-5095; Email: jessop@queensu.ca

Authors

Maedeh Ramezani − *Department of Chemistry and Department of Chemical Engineering, Queen's University, Kingston, ON K7L 3N6, Canada*

Sarah N. Ellis − *Department of Chemistry, Queen's University, Kingston, ON K7L 3N6, Canada*

Anna Riabtseva − *Department of Chemistry and Department of Chemical Engineering, Queen's University, Kingston, ON K7L 3N6, Canada*

Complete contact information is available at: https://pubs.acs.org/10.1021/acsomega.3c07644

Author Contributions

The manuscript was written through contributions of all authors. All authors have given approval to the final version of the manuscript.

Notes

The authors declare the following competing financial interest(s): P.G.J., M.F.C., and S.N.E. are inventors but not owners on patents and/or patent applications related to the technology.

ACKNOWLEDGMENTS

We gratefully acknowledge the support of the Natural Sciences and Engineering Research Council of Canada (NSERC, grant number STPGP 494487-16), the Canada Research Chairs Program (P.G.J.), and the Ontario Research Chairs Program (M.F.C.).

ABBREVIATIONS

AIBN=2,2′-azobis(2-methylpropionitrile)
Đ=dispersity
DMA=*N*,*N*-dimethylacrylamide
DMBS=2,4-dimethylbenzene sulfonate
DMO=direct membrane osmometry
ECP=external concentration polarization

https://doi.org/10.1021/acsomega.3c07644
ACS Omega 2023, 8, 49259−49269

FO=forward osmosis
FTIR=Fourier transform infrared spectroscopy
GPC=gel permeation chromatography
ICP=internal concentration polarization
LCST=lower critical solution temperature
LMH=flux as a function of volume and time (L m^{-2} h^{-1})
MBA=*N*,*N*′-methylenebisacrylamide
M_n=number average molecular weight
M_w=weight-average molecular weight
nBu-TAEA=*N*,*N*′,*N*″- *n*-butyryl tris(2-aminoethyl)amine
PAA Na=poly(acrylic acid) sodium salt
PAGB=poly (propylene glycol-ran-ethylene glycol) monobutyl ether
PDMA=poly(*N*,*N*-dimethylacrylamide)
PDMAAm=poly(*N*,*N*-dimethylallylamine)
PEG=poly(ethylene glycol)
PiBuCPMA=poly(*N*-(*N*′-isobutylcarbamido)propyl methacrylamide)
PNAAAM=poly(*N*-acryloylasparaginamide)
PNAGA=poly(*N*-acryloylglycinamide)
PNCPAM=poly(*N*-cyclopropylacrylamide)
PnPA=poly(*N*-*n*-propylacrylamide)
PiPA=poly(*N*-isopropylacrylamide)
PNIPAM-SA=poly(*N*-isopropylacrylamide-sodium acrylate)
PNIPAM-SSS=poly(sodium styrene-4-sulfonate-co-n-isopropylacrylamide)
PNVCL=poly(*N*-vinylcaprolactam)
l-PMEI=linear poly(*N*-methylethylenimine)
b-PMEI=branched poly(*N*-methylethylenimine)
PMAAm=poly(methacrylamide)
PMT=poly[{2-(methacryloyloxy)ethyl}trimethylammonium chloride]
P(MTEO)=[2-(methacryloyloxy)ethyl]- trimethylammonium chloride with 2-(2-methoxyethoxy) ethyl methacrylate
RO=reverse osmosis
RSF=reverse salt flux
trDDM=*tert*-dodecylmercaptan
TFA=trifluoroacetate
TMA=trimethylamine
π_{air}=osmotic pressure of the solution under air
π_{CO2}=osmotic pressure of the solution under 1 bar of CO_2

REFERENCES

(1) McCutcheon, J. R.; McGinnis, R. L.; Elimelech, M. Desalination by ammonia−carbon dioxide forward osmosis: Influence of draw and feed solution concentrations on process performance. *J. Membr. Sci.* **2006**, *278*, 114−123.
(2) Ezugbe, E.; Kweinor Tetteh, E.; Rathilal, S.; Asante-Sackey, D.; Amo-Duodu, G. Desalination of Municipal Wastewater Using Forward Osmosis. *Membranes* **2021**, 119−131.
(3) Tong, T.; Elimelech, M. The Global Rise of Zero Liquid Discharge for Wastewater Management: Drivers, Technologies, and Future Directions. *Environ. Sci. Technol.* **2016**, *50*, 6846−6855.
(4) Gao, Y.; Yu, M. Assessment of the economic impact of South-to-North Water Diversion Project on industrial sectors in Beijing. *J. Econ. Struct.* **2018**, *7*, 1−17.
(5) Grant, S. B.; Saphores, J. D.; Feldman, D. L.; Hamilton, A. J.; Fletcher, T. D.; Cook, P. L.; Stewardson, M.; Sanders, B. F.; Levin, L. A.; Ambrose, R. F.; Deletic, A.; Brown, R.; Jiang, S. C.; Rosso, D.; Cooper, W. J.; Marusic, I. Taking the "Waste" Out of "Wastewater" for Human Water Security and Ecosystem Sustainability. *Science.* **2012**, *337*, 681−686.
(6) Cui, H.; Zhang, H.; Yu, M.; Yang, F. Performance evaluation of electric-responsive hydrogels as draw agent in forward osmosis desalination. *Desalination.* **2018**, *426*, 118−126.
(7) Medina, B. G.; Garcia, A. Concentration of orange juice by reverse osmosis. *J. Food Process Eng.* **1988**, *10*, 217−230.
(8) Jesus, D. F.; Leite, M. F.; Silva, L. F. M.; Modesta, R. D.; Matta, V. M.; Cabral, L. M. C. Orange (Citrus sinensis) juice concentration by reverse osmosis. *J. Food Eng.* **2007**, *81*, 287−291.
(9) Haupt, A.; Lerch, A. Forward Osmosis Application in Manufacturing Industries: A Short Review. *Membranes.* **2018**, *8* (1−33), 47.
(10) Johnson, D. J.; Suwaileh, W. A.; Mohammed, A. W.; Hilal, N. Osmotic's potential: An overview of draw solutes for forward osmosis. *Desalination* **2018**, *434*, 100−120.
(11) Haddad, A. Z.; Menon, A. K.; Kang, H.; Urban, J. J.; Prasher, R. S.; Kostecki, R. Solar Desalination Using Thermally Responsive Ionic Liquids Regenerated with a Photonic Heater. *Environ. Sci. Technol.* **2021**, *55*, 3260−3269.
(12) Shaffer, D. L.; Werber, J. R.; Jaramillo, H.; Lin, S.; Elimelech, M. Forward osmosis: Where are we now? *Desalination.* **2015**, *356*, 271−284.
(13) Li, X.; Sakai, T. *Physics of Polymer Gels, Mass Transport in Polymer Gels*; 1 Edition. Edited by Sakai, T. Wiley-VCH Verlag GmbH & Co. KGaA, 2020; pp 137-150
(14) Cath, T. Y.; Childress, A. E.; Elimelech, M. Forward osmosis: Principles, applications, and recent developments. *J. Membr. Sci.* **2006**, *281*, 70−87.
(15) Suwaileh, W.; Pathak, N.; Shon, H.; Hilal, N. Forward osmosis membranes and processes: A comprehensive review of research trends and future outlook. *Desalination.* **2020**, *485*, 114455−114476.
(16) Ray, S. S.; Chen, S. S.; Sangeetha, D.; Chang, H. M.; Thanh, C. N. D.; Le, Q. H.; Ku, H. M. Developments in forward osmosis and membrane distillation for desalination of waters. *Environ. Chem. Let.* **2018**, *16*, 1247−1265.
(17) Kim, J.; Kim, J.; Lim, J.; Hong, S. Evaluation of ethanol as draw solute for forward osmosis (FO) process of highly saline (waste) water. *Desalination* **2019**, *456*, 23−31.
(18) McCutcheon, J. R.; McGinnis, R. L.; Elimelech, M. Desalination by ammonia−carbon dioxide forward osmosis: influence of draw and feed solution concentrations on process performance. *J. Membr. Sci.* **2006**, *278* (1−2), 114−123.
(19) Alabi, A.; Zou, L.; Graphene oxide/alginate/polyacrylate hydrogels as a draw agent for osmosis water purification. *Environ. Sci. Water Res. Technol*, **2023**. Doi: *9*, 3446, .
(20) Li, X.; Loh, C. H.; Wang, R.; Widjajanti, W.; Torres, J. Fabrication of a robust high-performance FO membrane by optimizing substrate structure and incorporating aquaporin into selective layer. *J. Membr. Sci.* **2017**, *525*, 257−268.
(21) Khan, B. E.; Mahmood, A.; Zaman, M.; Lee, K. H. Zinc sulfate as a draw solute in forward osmosis and its regeneration by reagent precipitation. *Desalination* **2024**, *571*, No. 117087.
(22) Na, Y.; Yang, S.; Lee, S. Evaluation of citrate-coated magnetic nanoparticles as draw solute for forward osmosis. *Desalination* **2014**, *347*, 34−42.
(23) Ban, I.; Drofenik, M.; Bukšek, H.; Petrinic, I.; Helix-Nielsen, C.; Vohl, S.; Gyergyek, S.; Stergar, J. Synthesis of magnetic nanoparticles with covalently bonded polyacrylic acid for use as forward osmosis draw agents. *Environ. Sci.: Water Research & Tech.* **2023**, *9*, 442−453.
(24) Bayrami, A.; Bagherzadeh, M.; Navi, H.; Nikkhoo, M.; Amini, M. Zwitterion-functionalized MIL-125-NH 2-based thin-film nanocomposite forward osmosis membranes: Towards improved performance for salt rejection and heavy metal removal. *New J. Chem.* **2022**, *46*, 15205−15218.
(25) Joafshan, M.; Shakeri, A.; Razavi, S. R.; Salehi, H. Gas responsive magnetic nanoparticle as novel draw agent for removal of Rhodamine B via forward osmosis: High water flux and easy regeneration. *Sep. Purif. Technol.* **2022**, *282*, No. 119998.
(26) Ge, Q.; Ling, M.; Chung, T. S. Draw solutions for forward osmosis processes: Developments, challenges, and prospects for the future. *J. Membr. Sci.* **2013**, *442*, 225−237.

https://doi.org/10.1021/acsomega.3c07644
ACS Omega 2023, 8, 49259−49269

(27) Achilli, A.; Cath, T. Y.; Childress, A. E. Selection of inorganic-based draw solutions for forward osmosis applications. *J. Membr. Sci.* **2010**, *364*, 233−241.
(28) Loeb, S.; Titelman, L.; Korngold, E.; Freiman, J. Effect of porous support fabric on osmosis through a Loeb-Sourirajan type asymmetric membrane. *J. Membr. Sci.* **1997**, *129*, 243−249.
(29) Cai, Y.; Hu, M. X. A critical review on draw solutes development for forward osmosis. *Desalination.* **2016**, *391*, 16−29.
(30) Hsu, C. H.; Ma, C.; Bui, N.; Song, Z.; Wilson, A. D.; Kostecki, R.; Diederichsen, K. M.; McCloskey, B. D.; Urban, J. J. Enhanced Forward Osmosis Desalination with a Hybrid Ionic Liquid/Hydrogel thermoresponsive Draw Agent System. *ACS Omega* **2019**, *4*, 4296−4303.
(31) Gil, E. S.; Hudson, S. M. Stimuli-responsive polymers and their bioconjugates. *Prog. Polym. Sci.* **2004**, *29*, 1173−1222.
(32) Zhao, Q.; Chen, N.; Zhao, D.; Lu, X. thermoresponsive Magnetic Nanoparticles for Seawater Desalination. *ACS. Appl. Mater. Interfaces.* **2013**, *5*, 11453−11461.
(33) Shi, Y.; Liao, X.; Chen, R.; Ge, Q. pH-Responsive Polyoxometalates that Achieve Efficient Wastewater Reclamation and Source Recovery via Forward Osmosis. *Environ. Sci. Technol.* **2021**, *55*, 12664−12671.
(34) Ellis, S. N.; Cunningham, M. F.; Jessop, P. G. Forward osmosis hydrogel draw agent that responds to both heat and CO_2. *Desalination.* **2021**, *510*, No. 115074.
(35) Ellis, S. N.; Riabtseva, A.; Dykeman, R. R.; Hargreaves, S.; Robert, T.; Champagne, P.; Cunningham, M. F.; Jessop, P. G. Nitrogen rich CO_2-responsive polymers as forward osmosis draw solutes. *Ind. Eng. Chem. Res.* **2019**, *58*, 22579−22586.
(36) Riabtseva, A.; Ellis, S. N.; Champagne, P.; Jessop, P. G.; Cunningham, M. F. CO_2-responsive branched polymers for forward osmosis applications: The effect of branching on draw solute properties. *Ind. Eng. Chem. Res.* **2021**, *60*, 9807−9816.
(37) Ullner, M.; Qamhieh, K.; Cabane, B. Osmotic pressure in polyelectrolyte solutions: cell-model and bulk simulations. *Soft. Matter.* **2018**, *14*, 5832−5846.
(38) Money, N. P. Osmotic pressure of aqueous polyethylene glycols: relationship between molecular weight and vapor pressure deficit. *Plant Physiol.* **1989**, *91*, 766−769.
(39) Cai, Y.; Shen, W.; Wang, R.; Krantz, W. B.; Fane, A. G.; Hu, X. CO_2 switchable dual responsive polymers as draw solutes for forward osmosis desalination. *Chem. Commun.* **2013**, *49*, 8377−8379.
(40) Yasukawa, M.; Tanaka, Y.; Takahashi, T.; Shibuya, M.; Mishima, S.; Matsuyama, H. Effect of molecular weight of draw solute on water permeation in forward osmosis process.″. *Ind. Eng. Chem. Res.* **2015**, *54*, 8239−8246.
(41) Grattoni, A.; Canavese, G.; Montevecchi, F. M.; Ferrari, M. Membrane osmometer as Alternative to Freezing Point and Vapor Pressure osmometry. *Anal. Chem.* **2008**, *80*, 2617−2622.
(42) Ellis, S. N.; Cunningham, M. F.; Jessop, P. G. A forward osmosis hydrogel draw agent that responds to both heat and CO_2. *Desalination* **2021**, *510*, No. 115074.
(43) Bhattacharyya, A.; O'Bryan, C.; Ni, Y.; Morley, C. D.; Taylor, C. R.; Angelini, T. E. Hydrogel compression and polymer osmotic pressure. *Biotribology.* **2020**, *22*, No. 100125.
(44) Madden, M. J.; Ellis, S. N.; Riabtseva, A.; Wilson, A. D.; Cunningham, M. F.; Jessop, P. G. Comparison of vapour pressure osmometry, freezing point osmometry and direct membrane osmometry for determining the osmotic pressure of concentrated solutions. *Desalination* **2022**, *539*, No. 115946.
(45) Kakehashi, R.; Yamazoe, H.; Maeda, H. Osmotic Coefficients of Vinylic Polyelectrolyte Solutions without Added Salt. *Colloid Polym. Sci.* **1998**, *276*, 28−33.
(46) Inada, A.; Kumagai, K.; Matsuyama, H. Effect of the molecular weights of thermoresponsive polyalkylene glycol draw solutes on forward osmosis performance. *Sep. Purif. Technol.* **2020**, *252*, No. 117462.
(47) Ahmed, M.; Kumar, R.; Garudachari, B.; Thomas, J. P. Performance evaluation of a thermoresponsive polyelectrolyte draw solution in a pilot scale forward osmosis seawater desalination system. *Desalination* **2019**, *452*, 132−140.
(48) Ge, Q.; Su, J.; Amy, G. L.; Chung, T. S. Exploration of polyelectrolytes as draw solutes in forward osmosis processes. *Water Res.* **2012**, *46*, 1318−1326.
(49) Zhao, D.; Wang, P.; Zhao, Q.; Chen, N.; Lu, X. thermoresponsive copolymer-based draw solution for seawater desalination in a combined process of forward osmosis and membrane distillation. *Desalination.* **2014**, *348*, 26−32.
(50) Boo, C.; Khalil, Y. F.; Elimelech, M. Performance evaluation of trimethylamine−carbon dioxide thermolytic draw solution for engineered osmosis. *J. Membr. Sci.* **2015**, *473*, 302−309.
(51) Russell, T. P. Surface-responsive materials. *Science* **2002**, *297*, 964−967.
(52) Roy, D.; Brooks, W. L.; Sumerlin, B. S. New directions in thermoresponsive polymers. *Chem. Soci. Rev.* **2013**, *42*, 7214−7243.
(53) Hansen, C. M. The universality of the solubility parameter. *I&EC Prod. Res. Dev.* **1969**, *8*, 2−11.
(54) Shahamat, M.; Rey, A. D. Molecular thermodynamic characterization of LCST fluid phase behavior and exploring electrostatic algorithms to compute polymer/solvent solubility parameters in the canonical ensemble. *Polymer* **2013**, *54*, 4997−5004.
(55) Venkatram, S.; Kim, C.; Chandrasekaran, A.; Ramprasad, R. Critical assessment of the Hildebrand and Hansen solubility parameters for polymers. *J. Chem. Inf. Model.* **2019**, *59*, 4188−4194.
(56) Li, S.; Feng, L.; Lu, H.; Feng, S. From LCST to UCST: the phase separation behaviour of thermo-responsive polysiloxanes with the solubility parameters of solvents. *New J. Chem.* **2017**, *41*, 1997−2003.
(57) Miller-Chou, B. A.; Koenig, J. L. A review of polymer dissolution. *Prog. Polym. Sci.* **2003**, *28*, 1223−1270.
(58) Lessard, D. G.; Ousalem, M.; Zhu, X. X. Effect of the molecular weight on the lower critical solution temperature of poly (N, N-diethylacrylamide) in aqueous solutions. *Can. J. Chem.* **2001**, *79*, 1870−1874.
(59) Schild, H. G.; Muthukumar, M.; Tirrell, D. A. Cononsolvency in mixed aqueous solutions of poly (N-isopropylacrylamide). *Macromolecules* **1991**, *24*, 948−952.
(60) Lutz, J. F.; Akdemir, Ö.; Hoth, A. Point by Point Comparison of Two Thermosensitive Polymers Exhibiting a Similar LCST: Is the Age of Poly (NIPAM) Over?″. *J. Am. Chem. Soc.* **2006**, *128*, 13046−13047.
(61) Ou, R.; Wang, Y.; Wang, H.; Xu, T. thermo-sensitive polyelectrolytes as draw solutions in forward osmosis process. *Desalination* **2013**, *318*, 48−55.
(62) Tong, Z.; Zeng, F.; Zheng, X.; Sato, T. Inverse molecular weight dependence of cloud points for aqueous poly (N-isopropylacrylamide) solutions. *Macromolecules* **1999**, *32*, 4488−4490.
(63) Otake, K.; Karaki, R.; Ebina, T.; Yokoyama, C.; Takahashi, S. Pressure effects on the aggregation of poly (N-isopropylacrylamide) and poly (N-isopropylacrylamide-co-acrylic acid) in aqueous solutions. *Macromolecules* **1993**, *26*, 2194−2197.
(64) Zheng, X.; Tong, Z.; Xie, X.; Zeng, F. Phase separation in poly (N-isopropyl acrylamide)/water solutions I. Cloud point curves and microgelation. *Polym. J.* **1998**, *30*, 284−288.
(65) Tiktopulo, E. I.; Uversky, V. N.; Lushchik, V. B.; Klenin, S. I.; Bychkova, V. E.; Ptitsyn, O. B. ″ Domain″ Coil-Globule Transition in Homopolymers. *Macromolecules* **1995**, *28*, 7519−7524.
(66) Zhang, Q.; Weber, C.; Schubert, U. S.; Hoogenboom, R. thermoresponsive polymers with lower critical solution temperature: from fundamental aspects and measuring techniques to recommended turbidimetry conditions. *Mater. Horiz.* **2017**, *4*, 109−116.
(67) Schild, H. G.; Tirrell, D. A. Microcalorimetric detection of lower critical solution temperatures in aqueous polymer solutions. *J. Phys. Chem.* **1990**, *94*, 4352−4356.
(68) Berg, A. V. D.; Perkins, T.; Isselhardt, M. Effects of Sap Concentration with Reverse Osmosis on Syrup Composition and Flavor. *Maple Digest.* **2015**, *54*, 11−33.

https://doi.org/10.1021/acsomega.3c07644
ACS Omega 2023, 8, 49259−49269

(69) Idziak, I.; Avoce, D.; Lessard, D.; Gravel, D.; Zhu, X. X. Thermosensitivity of aqueous solutions of poly (N, N-diethylacrylamide). *Macromolecules* **1999**, *32*, 1260−1263.
(70) Arotçaréna, M.; Heise, B.; Ishaya, S.; Laschewsky, A. Switching the inside and the outside of aggregates of water-soluble block copolymers with double thermoresponsivity. *J. Am.Chem. Soc.* **2002**, *124*, 3787−3793.
(71) Gray, G. T.; McCutcheon, J. R.; Elimelech, M. Internal concentration polarization in forward osmosis: role of membrane orientation. *Desalination.* **2006**, *197*, 1−8.
(72) Lim, S.; Park, M. J.; Phuntsho, S.; Tijing, L. D.; Nisola, G. M.; Shim, W. G.; Chung, W. J.; Shon, H. K. Dual-layered nanocomposite substrate membrane based on polysulfone/graphene oxide for mitigating internal concentration polarization in forward osmosis. *Polymer* **2017**, *110*, 36−48.
(73) Yong, J. S.; Phillip, W. A.; Elimelech, M. Coupled reverse draw solute permeation and water flux in forward osmosis with neutral draw solutes. *J. Membr. Sci.* **2012**, *392*−*393*, 9−17.

https://doi.org/10.1021/acsomega.3c07644
ACS Omega 2023, 8, 49259−49269